Undulatory Delamination of Thin Polymer Films on Gold Surfaces

Soonwoo Chah,[†] Jaan Noolandi,[‡] and Richard N. Zare*[,†]

Department of Chemistry, Stanford University, Stanford, California 94305, Department of Chemical Engineering, Stanford University, Stanford, California 94305, and Department of Ophthalmology, Stanford University School of Medicine, Stanford, California 94305

Received: June 29, 2005; In Final Form: August 20, 2005

Using two-dimensional surface plasmon resonance measurements, we have observed the formation of traveling waves in the delamination of thin films of polydimethylsilane (PDMS) exposed to methanol. Films were spin-coated on a gold surface and the methanol was added to the top surface. The stress-induced instability caused by the swelling of the PDMS thin film when its edge is pinned to the gold surface leads to wrinkle formation and propagation at the interface. The periodic pattern is thought to be the result of an Asaro-Tiller-Grinfeld (ATG) instability.

Introduction

The morphology and properties of materials can be strongly influenced by elastic effects. If the nonequilibrium elastic energies build up in materials, such as in thin crystalline films, they will find ways to release these energies while evolving to an equilibrium state.[1] For example, thin solid films often have considerable intrinsic internal stress caused by the method of deposition. Such thin films may delaminate and buckle to release the stress.[2] Relatively few instances have been studied in detail, and they involve crystalline films.[3−6] We report on a similar phenomenon that occurs in polymeric thin films when they swell from exposure to solvent.

Using evanescent-wave spectroscopic techniques[7] we previously examined a thin film of polydimethylsilane (PDMS) on a solid gold surface as a solvent, methanol, penetrated into the film. We proposed that the delamination took place as a result of the swelling of the polymer as the solvent penetrated its structure. Because we were limited to one-dimensional analytical data, however, we could not determine how the stress was released at the interface. In this study, we employed surface plasmon resonance (SPR) microscopy[8−15] to investigate the polymer−gold interface with temporal and spatial resolution. The SPR images provide strong evidence that as methanol permeates and swells the polymer, the surface suddenly undergoes oscillatory wave motion as it partially detaches from the gold substrate. This phenomenon is illustrated schematically in Figure 1. A theoretical analysis suggests that the process shown in Figure 1 is being driven by the Asaro−Tiller−Grinfeld (ATG) instability,[16−18] previously only observed at crystalline interfaces.

Experimental Methods

Preparation of PDMS Thin Film on Gold Surfaces. A microscope slide (3×1 in.^{2} SF10 glass, Schott Glass Technology) was immersed in a piranha solution (sulfuric acid:hydrogen peroxide 70:30 vol %) for 2 min. It was copiously washed with purified water (>18 MΩ cm) several times and dried with nitrogen gas. Then, a 50 nm gold film following a 1 nm Cr adhesive layer was deposited on the clean SF10 glass under high vacuum ($5-6 \times 10^{-7}$ mbar) by an evaporator (Auto 306, Edwards High Vacuum International). The thickness was controlled by using a quartz crystal microbalance (QCM) installed in the evaporator.

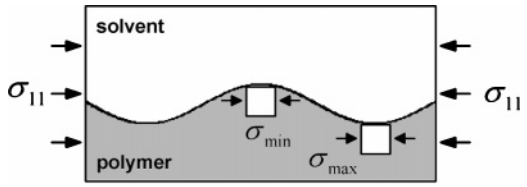

Figure 1. Schematic diagram showing the origin of the Asaro−Tiller−Grinfeld (ATG) instability for a uniaxial compressive stress σ_{11} applied at the polymer−solvent interface. The stress σ_{min} is lowest at the hills of the polymer density profile, and highest, σ_{max}, in the valleys. The stress concentration in the valleys, combined with the stress relaxation in the hills causes the amplitude of the profile to increase until nonlinear elasticity eventually stabilizes the interface.

We followed a procedure for preparing PDMS film on the gold surface described previously.[7] GE Silicones components RTV615A (linear polymer) and RTV615B (containing cross-linking agent) were combined in a 10:1 (wt %) ratio and mixed thoroughly for 2 min. The mixture was degassed in a vacuum desiccator for an hour. It was then spin-coated onto the gold-coated glass. We cured the polymer film at 80 °C for 3 h in an oven. The film was cut vertically, and its cross section was suspended over the stage of a microscope (Zeiss Axiovert 135) arranged to project onto a monitor screen. The width of the cross section as measured on the monitor screen was converted to microns by calibrating with a stage micrometer (Pyser-SGI Limited). The thickness of the polymer film was around 100 m, which is much greater than the penetration depth (~200 nm) of the evanescent wave.

Surface Plasmon Resonance (SPR) Setup. The angle-resolved and time-resolved SPR measurements were carried out with a home-built SPR setup based on Kretschmann configuration.[19−24] Figure 2 shows a schematic diagram of the SPR instrument used in this work. A polymer spin-coated gold substrate was attached to a SF10 prism ($n = 1.72825$, 1.5×1.5 cm^2 right angle prism, Esco Products, Inc.) with index

* Address correspondence to this author. E-mail: zare@stanford.edu.
[†] Department of Chemistry, Stanford University.
[‡] Department of Chemical Engineering, Stanford University, and Department of Ophthalmology, Stanford University School of Medicine.

10.1021/jp0535644 CCC: $30.25
Published on Web 09/24/2005

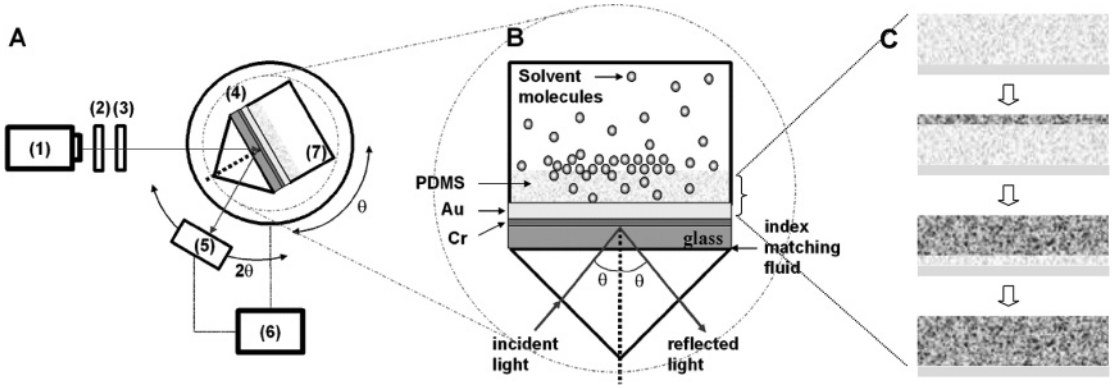

Figure 2. (A) Schematic diagram of a surface plasmon resonance (SPR) setup. Incoming light is reflected to a detector by the gold film, which is evaporated on SF10 glass, following the deposition of a thin binding layer of Cr. When the rotation stage turns by an angle θ, the detector moves 2θ: (1) laser, (2) polarizer, (3) convex lens, (4) rotation stage, (5) detector, (6) computer, and (7) Teflon cell. (B) Enlargement of a reaction cell. The gold surface is spin-coated with polydimethylsilane (PDMS) with a thickness of ~100 μm. For the diffusion of methanol into PDMS, the solution is injected into a Teflon cell. Then, the effect of solvent diffusion on the SPR signal is examined as a function of time. Part C shows the ideal diffusion of methanol into the PDMS film.

matching fluid ($n = 1.730 \pm 0.0005$, R. P. Cargille Laboratories, Inc.). A Teflon cell was attached to the gold substrate to hold solutions. The 658-nm output of a 30-mW diode laser (LDCU5/4953, Power Technologies) was p-polarized and focused by a lens ($f = 50$ cm) through the prism onto the gold substrate. The cell had an O-ring (ID = 0.6 cm, not shown in Figure), and the incoming laser light contacted the solution in the middle of the O-ring. Both the prism and the cell were mounted on a rotating plate (two-circle goniometer 415, Huber) to control the angle of the incident light. The light reflected from the gold substrate was viewed by a photodiode detector (201/579-7227, Thorlabs Inc) for averaged 1-D data and a camera (C2400-08, Hamamatsu) for 2-D data. The operation of the stepping motors, data acquisition, and analysis were carried out with a home-written program.

We initially recorded angle-resolved SPR curves for a PDMS-coated gold surface. Then we injected methanol into the flow cell and recorded SPR data at several time intervals while the methanol penetrated the polymer layer. Figure 2C shows the ideal diffusion of methanol into the polymer layer. After the 1-D SPR measurement, we replaced a single-cell photodiode detector with a camera, and measured the two-dimensional image for the same system. The sample and the detector were fixed at 65° and 130°, respectively. The polymer region appears as white with ~0.7 reflectivity while the methanol area appears as black with ~0.0 reflectivity.

Results and Discussion

Thin Film Delamination: *1-D SPR Data.* The far right of Figure 3 (■) shows a representative angle-resolved SPR curve for a PDMS. The position of the SPR angle near 78° is, within error, what is expected from the published refractive index of 1.415. The other curves in Figure 3 show SPR data for the PDMS system at five different time intervals after injection of methanol above the film. Initially, the PDMS characteristic curve shifts to the left. Then it increases in its reflectivity at the SPR angle and disappears. A second peak around 65° appears and grows, showing an isotropic point around 70° until it stops at a certain stabilized point. The curve change is characterized by two phenomena. One is the initial shift to the left, and the other is the disappearance of the first peak accompanied by the appearance of the second peak.

The shift to the left of the PDMS peak arises from either an ideal diffusion of methanol into PDMS or an insertion of a thin, homogeneous layer of methanol that has permeated the PDMS

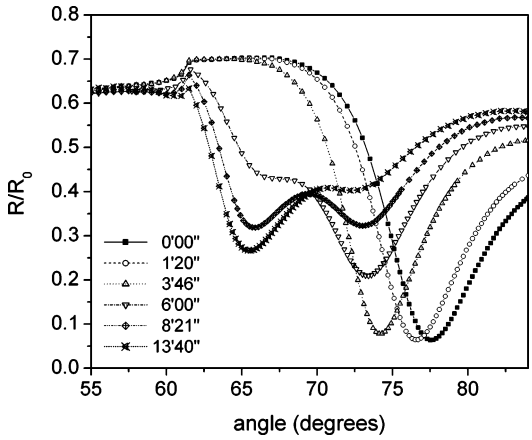

Figure 3. Angle-resolved surface plasmon resonance curves for diffusion of methanol through a PDMS film. Individual curves show the SPR signal for a ~100-μm-thick film of PDMS recorded at each time indicated.

and separated the gold surface from the polymer layer. The shift possibly results from a combination of both phenomena. Figure 4A illustrates the schematic and theoretical calculation of SPR for the first case. The SPR curve for pure methanol appears around 65° in a manner similar to that for the PDMS layer (not shown here), which indicates that its refractive index is 1.329. Assuming that the ideal diffusion occurs in the film without any additional change at the interface, we can expect the optical property or dielectric constant of the film to decrease proportionally to the extent of methanol diffusion into the pores of the polymer layer. Consequently, the SPR signal is expected to shift to the left from the initial peak as much as the polymer film becomes soaked by methanol over the interface. Theoretical calculation based on the Fresnel equation supports this idea as shown on the right side of Figure 4A. We calculated the SPR curves as a function of the refractive index of the methanol-soaked PDMS layer. As the refractive index decreases, the curve shifts to the left and is accompanied by a decrease in the critical angle. The shift of the PDMS peak to the left also can be caused by insertion of methanol layer at the interface. The SPR data on the right side of Figure 4B show the theoretical curve-shift as a function of thickness of the homogeneous methanol layer at the interface. The thicker the layer is, the more it shifts to the left. The extent of the shift in Figure 4B, however, is not proportional to the thickness as it is to dielectric constant in Figure 4A. We find that a layer thicker than 300 nm may be

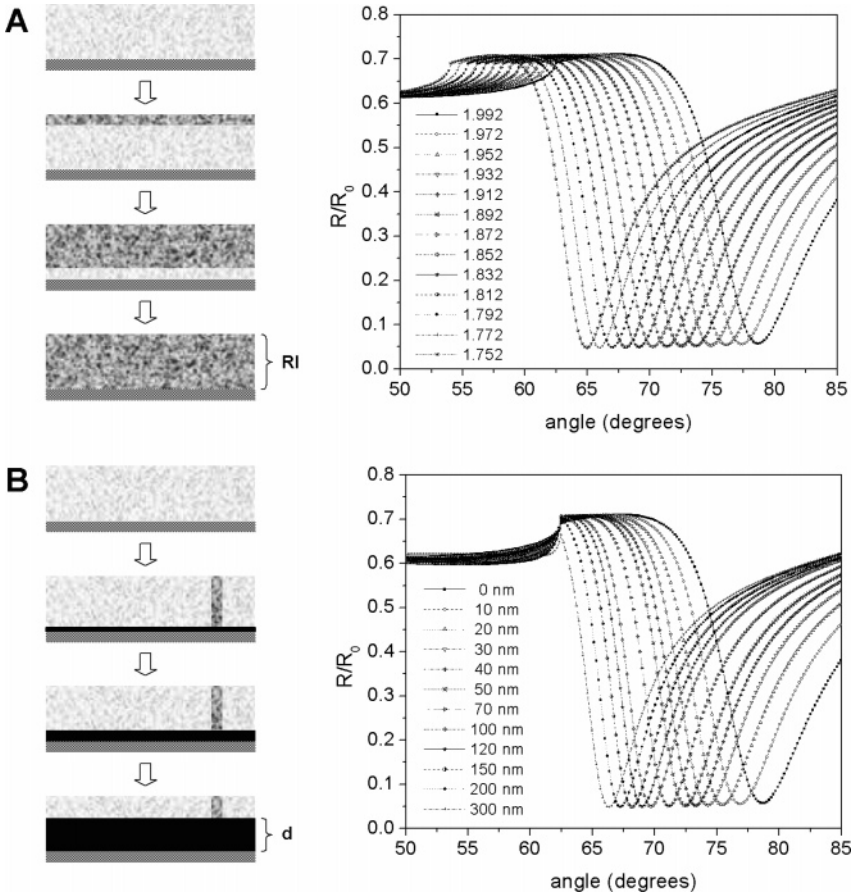

Figure 4. (A) schematic diagram of ideal diffusion of methanol into the evanescent range of the PDMS layer and its theoretical SPR data calculated as a function of dielectric constant (= RI^2). The refractive index (RI) of the PDMS proportionally changes as the methanol penetrates the polymer. Consequently, the curves shift to the left in proportion to the RI change. (B) Schematic diagram illustrating the formation of an homogeneous methanol layer between polymer film and gold surface, and its theoretical SPR data calculated as a function of thickness *d* of permeated methanol. As the thickness of methanol layer at the interface increases, the curve shifts to the left. The extent of the shift gradually decreases.

regarded as a pure methanol layer without any contribution from PDMS on top. In addition, it is noted that the critical angle does not change appreciably as in the case of Figure 4A. Comparing the two cases with the experimental data in Figure 3, we can conclude that initial left-shift is closer to the second case. In other words, the methanol initially begins to penetrate from the weakest point, and reaches the interface resulting in a ~40 nm homogeneous methanol layer in 3 min and 46 s.

Curves after the third measurement (data after 3′ 46″), however, accompany unexpected movement, which is the growth of the second peak. This peak occurs at the same angle as the pure methanol SPR angle (~65°). The presence of two SPR peaks in a single angle-resolved curve is very uncommon and indicates that two distinct populations of molecules must be present and horizontally separated from one another above the illumination region (~1 mm) of the substrate.[7] The ~40 nm homogeneous methanol layer formed locally at the early stage of diffusion becomes thicker to form a ~300 nm methanol layer at the interface resulting in a delamination of PDMS film. If this growth in the methanol layer occurs homogeneously over the interface, the SPR will shift as shown in Figure 4B. However, because it is generated locally from several spots, two characteristic peaks showing an isotropic point are simultaneously seen in the signal. The peak at ~65° provides evidence that in an area of the illumination region, the PDMS has delaminated from the substrate surface to the extent that only bulk methanol covers the region of the evanescent field above the SPR substrate. The remaining peak at ~75° shows that some PDMS still remains attached to the SPR substrate surface or has been delaminated only slightly by a thin, homogeneous layer of methanol. This delamination is attributed to the swelling and penetration of the polymer by the solvent. The polymer layer is constrained around the edges by the pressure of the flow cell; therefore, when it swells with solvent, it is likely to lift off the surface of the substrate. Considering the delamination at the interface, in Figure 3 the reflectivity ratio of the first (~65°) to the second (~75°) peak is expected to show the ratio of polymer region to methanol region.

2-D SPR Data. The SPR image for one spot was monitored as a function of time after the injection of methanol over the PDMS layer to determine how the stress was released at the interface. Figure 5 presents representative 2-D SPR images for the delaminated surface.[25] Initially, the surface has high reflectivity at 65° because the SPR angle for the PDMS layer appears around 78° (I in Figure 5). The injection of methanol over the polymer film causes the inhomogeneous diffusion of methanol (II and III in Figure 5). The methanol reaches the interface from one spot, permeates along the interface, and forms a locally homogeneous and thin (~40 nm) layer. The reflectivity at the fixed angle still remains because the SPR peaks slightly shift in SPR angle without any change of reflectivity at 65° (IV in Figure 5, initial curve shift in Figure 3). When the delamination begins at the interface, the surface turns black at some spots and gradually extends in area until it is stabilized (V-1 ~ V-4 in Figure 5). The step V results in the decrease of the first peak accompanied by the increase of the second peak in Figure 3.

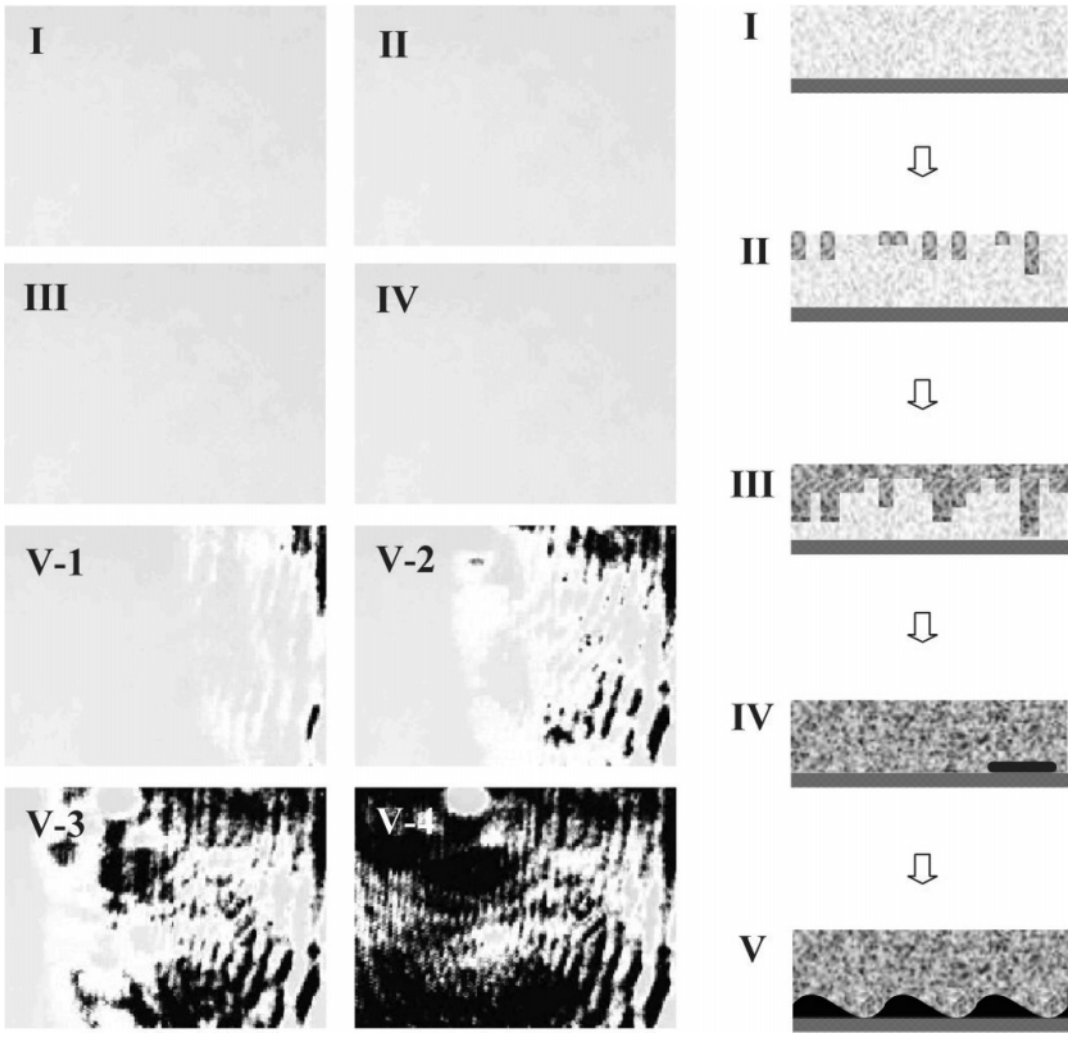

Figure 5. Two-dimensional SPR image as a function of time after the injection of methanol over the polymer film and a schematic diagram illustrating its idealized behavior at each step. The surface shows high reflectivity until the methanol reaches the interface (I, II, III) and forms a thin (~40 nm) and homogeneous methanol layer at the interface (IV). When the polymer layer starts being delaminated (V), the surface changes to black and gradually extends in area until it reaches some from of stabilization.

We find that the stress is released uniaxially from a methanol-inserted spot by delamination. It is important to note that the wrinkle wavelengths are much larger (~30 μm) than the lattice spacing or molecular size, indicating that the wrinkles are not merely artifacts of the lattice geometry. We conducted at least three SPR trials for the injection of methanol onto PDMS films. From one trial to the next, the extent to which the peaks shift and the relative sizes of the peaks for 1-D SPR and the images for 2-D SPR vary; however, two SPR peaks and both regions appear for all trials.

Theoretical Analysis. We believe that our observations are a manifestation of a stress-induced kinetically driven morphological instability leading to strain relief at the free PDMS−methanol interface of the non-hydrostatically stressed polymer. This mechanism for the release of nonequilibrium elastic energy, also known as the Asaro−Tiller−Grinfeld (ATG) instability, has been observed during solid-phase epitaxial growth in pure Si(001) for the case of stress applied parallel to the amorphous−crystal interface[26] and also during the polymerization of single-crystal films of polydiacetylene in epitaxy with their monomer substrate.[27] In the latter case polymerization induces a uniaxial stress and leads to the formation of several types of wrinkle patterns on the surface of the polymer.

In our experiment the uniaxial stress at the PDMS−methanol interface is generated by the expansion of the polymer, which, as explained earlier, is pinned at the edge of the O-ring used to fasten the polymer film to the gold surface. After the methanol is added to the surface of the PDMS, a fairly regular delamination pattern as shown in Figure 5 appears on the surface of the polymer. The strain relief mechanism moves material differentially from valleys to hills buckling at a given wavenumber depending on the elastic properties of the material, as illustrated in Figure 1. Although stress relaxation takes place at the hills and increases at the valleys, as explained later these two effects do not cancel because of the asymmetry of the system and there is an overall reduction in the elastic energy of the polymer near the surface. Consequently the stress concentrations in the valleys slow the motion of the valleys relative to the hills causing the amplitude of the instability to grow until nonlinear elastic effects halt the process. In addition there is a reduction in the surface free energy of the PDMS−methanol interface because methanol is a good solvent for PDMS. Next we discuss the theory in more formal terms.

A comprehensive theoretical treatment of surface instabilities induced by stress, including the Grinfeld instability, has been developed by Müller and Grant.[4] Their model is based on a

coarse-grained Ginzburg−Landau free energy F in which the elastic strain is a subsidiary tensor variable coupled to a nonconserved scalar order parameter,

$$F(\phi,u_{ij}) = \int \mathrm{d}^3 r[f(\phi,u_{ij}) + (l/2)|\nabla\phi|^2] \quad (1)$$

where

$$u_{ij} = \frac{1}{2}\left(\frac{\partial u_i}{\partial x_j} + \frac{\partial u_j}{\partial x_i}\right) \quad (2)$$

where u_{ij} is the strain, u_i is the displacement field from a reference state, ϕ is the order parameter, l is a constant (proportional to the surface tension), and $f(\phi,u_{ij})$ is the bulk elastic free energy. The details of the solution of the model for uniaxial stress are given in the paper by Müller and Grant,[4] as well as in the thesis of Judith Müller.[28] For our purpose we point out that with the appropriate boundary conditions at and near the surface, a linear stability analysis can be used to characterize the dynamics of a small amplitude sinusoidal surface profile,

$$h(x,t) = h(t)\sin(qx) \quad (3)$$

Solving for the stress state at the interface with the appropriate boundary conditions gives

$$h(t) = h_0 \exp(\omega t) \quad (4)$$

Here ω describes the normal-mode growth rate, with the dispersion relation given by

$$\omega(q) = Aq^3 - \gamma Bq^4 \quad (5)$$

for the case of surface diffusion. Here A and B are positive constants and q is the mode wave vector. For a good solvent the surface tension γ is negative, so that for our system all wave vectors are unstable with respect to small perturbations of the surface, unlike the case for positive surface tension, where some modes for which $q > q_c$ are stable and the other modes for which $q < q_c$ are unstable. The above analysis assumes that the elastic field relaxes much faster than the order parameter ϕ. The elastic field can then be solved in terms of the order parameter with the condition of local mechanical equilibrium. If this is not the case one has to use the theory of elasticity fluid-infiltrated porous solids (poroelasticity)[29] and the analysis becomes much more complicated.

In summary, for uniaxial stress, when the surface is perturbed the applied stress results in a nonuniform stress distribution in which stress relaxation occurs in the hills, and a higher stress concentration takes place in the valleys. The resulting stress gradient along the surface drives a mass flow from the valleys to the hills. It is important to note that the amount of stress relaxation gained in the hills is not offset by the increase in stress in the valleys. This is because the asymmetry of the system, with the solvent on one side of the surface and the bulk on the other side, allows some of the stress near the bulk phase to be dissipated, resulting in a net reduction of stress energy for the entire system. As the instability increases, the valleys become deeper and increase the stress gradient even more. Eventually the system is stabilized by the surface tension (if the surface tension is positive) or by higher order nonlinear elastic terms in the free energy (if the surface tension is negative, as in the case of PDMS and methanol).

Finally, it is clear that the negative surface tension alone cannot drive the instability, as opposed to the stress relaxation mechanism. This is because the interfacial surface energy is degenerate. For a given negative surface tension, the same interfacial free energy can be achieved by keeping the wavelength of the instability constant and increasing the amplitude, or by keeping the amplitude constant and decreasing the wavelength. In both cases the interfacial free energy is the same, because it is proportional to the amount of surface area. The stress relaxation mechanism lifts this degeneracy and determines a particular wavelength for the instability, according to the specific material and solvent properties under consideration.

Conclusions

We have investigated the delamination of PDMS films on gold surfaces using surface plasmon resonance spectroscopy. Diffusion of methanol into the polymer film causes swelling of the layer. Simultaneously, the heterogeneous polymer film results in an inhomogeneous penetration of methanol into its weakest points. A localized, homogeneous methanol layer is generated at the interface where methanol first arrives. The polymer becomes increasingly unstable as it soaks up methanol. Uniaxial stress at the PDMS−methanol interface is generated by the expansion of the polymer. The stress instability drives the morphological instability leading to strain relief at the interface, resulting in uniaxial propagation patterns on the surface. The stress relief mechanism of the polymer film can be understood in terms of the Asaro−Tiller−Grinfeld (ATG) instability theory. More studies need to be carried out to investigate this phenomenon and determine the factors that cause the propagation of surface waves.

Acknowledgment. This work is supported by the National Science Foundation under grant no. PHYS-0411641.

Supporting Information Available: A movie file showing the delamination in Figure 5. This material is available free of charge via the Internet at http://pubs.acs.org.

References and Notes

(1) Crosby, K. M.; Bradley, R. M. *Phys. Rev. E* **1988**, *59*, 2542−2545.
(2) Gioia, G.; Ortiz, M. *Adv. Appl. Mech.* **1997**, *33*, 119−192.
(3) Peyla, P. *Phys. Rev. E* **2000**, *62*, 1501−1504.
(4) Müller, J.; Grant, M. *Phys. Rev. Lett.* **1999**, *82*, 1736−1739.
(5) Ogawa, K.; Ohkoshi, T.; Takeuchi, T.; Mizoguchi, T.; Masumoto, T. *Jpn. J. Appl. Phys.* **1986**, *25*, 695−700.
(6) Gille, G.; Rau, B. *Thin Solid Films* **1984**, *120*, 109−121.
(7) Hannon, T. E.; Chah, S.; Zare, R. N. *J. Phys. Chem. B* **2005**, *109*, 7435−7442.
(8) Yeatman, E.; Ash, E. A. *Electron. Lett.* **1987**, *23*, 1091−1092.
(9) Yeatman, E.; Ash, E. A. *SPIE Scanning Microsc. Technol. Appl.* **1988**, *897*, 100−107.
(10) Rothenhausler, B.; Knoll, W. *Nature* **1988**, *332*, 615−617.
(11) Hickel, W.; Kamp, D.; Knoll, W. *Nature* **1989**, *339*, 186.
(12) Lyon, L. A.; Holliway, W. D.; Natan, M. J. *Rev. Sci. Instrum.* **1999**, *70*, 2076−2081.
(13) Brockman, J. M.; Nelson, B. P.; Corn, R. M. *Annu. Rev. Phys. Chem.* **2000**, *51*, 41−63.
(14) Johansen, K.; Arwin, H.; Lundström, I.; Liedberg, B. *Rev. Sci. Instrum.* **2000**, *71*, 3530−3538.
(15) Shumaker-Parry, J. S.; Campbell, C. T. *Anal. Chem* **2004**, *76*, 907−917.
(16) Asaro, R. J.; Miller, W. A. *Metall. Trans.* **1972**, *3*, 1789−1796.
(17) Grinfeld, M. A. *Sov. Phys. Dokl.* **1986**, *31*, 831−834.
(18) Srolovitz, D. J. *Acta Metall.* **1981**, *37*, 621−625.
(19) Kretschmann, E. *Z. Phys.* **1971**, *241*, 313.
(20) Raether, H. *Surface Plasmons on Smooth and Rough Surfaces and Gratings*; Springer Tracts in Modern Physics, Vol. 111; Springer-Verlag: Berlin, Germany, 1988.
(21) Peterlinz, K. A.; Georgiadis, R. *Langmuir* **1996**, *12*, 4731−4740.

(22) Boussaad, S.; Pean, J.; Tao, N. J. *Anal. Chem.* **2000**, *72*, 222−226.

(23) Hutter, E.; Fendler, J. H.; Roy, D. *J. Phys. Chem. B* **2001**, *105*, 11159−11168.

(24) Bailey, L. E.; Kambhampati, D.; Kanazawa, K. K.; Knoll, W.; Frank, C. W. *Langmuir* **2002**, *18*, 479−489.

(25) A movie file showing the delamination in Figure 5, delamination-.avi, is provided as Supporting Information. The length of the *x*-axis and PDMS thickness is 2 mm and 100 μm, respectively. The movie plays forty times faster than actual time.

(26) Barvosa-Carter, W.; Aziz, M. J.; Gray, L. J.; Kaplan, T. *Phys. Rev. Lett.* **1998**, *81* (7), 1445−1448.

(27) Berrhar, J.; Caroli, C.; Lapersonne-Meyer, C.; Schott, M. *Phys. Rev. B* **1992**, *46* (20), 13487−13495.

(28) Müller, J. Study of Stress-Induced Morphological Instabilities; Ph.D. Thesis, Centre for the Physics of Materials, Department of Physics, McGill University: Montreal, Quebec, Canada, 1998.

(29) Fairhurst, C. *Comprehensive Rock Engineering*: *Practice and Projects*; Vol. II, Analysis and Design Method, 1st ed.; Pergamon Press: New York, 1993; pp 113−171.